Biomarker-based H-Print quantifies the composition of mixed sympagic and pelagic algae consumed by *Artemia* sp.

Thomas A. Brown*,1 and Simon T. Belt

School of Geography, Earth and Environmental Sciences, University of Plymouth, Plymouth, UK, PL4 8AA

* Corresponding author: thomas.brown@sams.ac.uk

[1] Current address: Department of Marine Ecology and Chemistry, Scottish Association for Marine Science, Oban, UK, PA37 1QA. (Thomas.Brown@sams.ac.uk)

Abstract

Quantifying the importance of sea ice microalgae as a food source in Arctic ecosystems is becoming an increasingly important research objective as sea ice extent and thickness continue to reduce. Recently, the analysis of certain diatom-derived highly branched isoprenoid (HBI) lipid biomarkers has provided a means of qualitatively distinguishing between sympagic (sea ice) and pelagic algae in Arctic animals. By combining the abundances of these lipids into an HBI-fingerprint, or "H-Print", an estimate of the relative proportions of HBIs from each algal source can also be made. Although H-Print analysis of animal tissues in the Arctic is starting to provide such information, it has not yet been established to what extent H-Prints in animals provide a true reflection of the content of their algal food source. Here it is demonstrated that the H-Print determination can yield reliable

estimates of mixed sympagic/pelagic algal content both within a food source of known composition, and in a primary consumer fed on it. In doing so, the utility of the H-Print is extended towards providing quantitative estimates of the relative importance of sympagic algae to animal diet. To achieve this, a series of 5 algal samples were prepared with known %sympagic algal content ranging from 0 to 100%. Analysis of these samples led to a comparison of different regression models based upon H-Prints using 4 different combinations of individual HBIs. A linear model comprising 3 HBIs (2 sympagic and 1 pelagic) provided the most accurate estimates of the sympagic content (-1%, 50% and 101%) for samples containing 0%, 50% and 100% sympagic algae. This linear model was then used to estimate the proportion of sympagic algae in *Artemia* sp. (-3%, 44% and 101%) fed on the same algal mixtures in the laboratory. The similarity between H-Prints in mixed algae and *Artemia* sp. suggested that H-Prints were not altered substantially by grazing, and this was also confirmed by analysis of the remaining water (containing ungrazed algae and faecal pellets), where H-Prints were not significantly different from those obtained for the algae or *Artemia* sp. (p = >0.3). This study has extended the usefulness of the H-Print as an approach to determine ecosystem change in the future. Indeed, the ability of the H-Print to provide quantitative estimates of the importance of sympagic algae to Arctic animals is likely to result in valuable data that can be used for modelling the broader ecological impact of reducing sea ice extent.

Keywords: Highly branched isoprenoid (HBI), H-Print, sea ice algae, sympagic carbon, foodweb, Arctic

1 Introduction

Arctic sea ice provides a habitat for ice-adapted microalgae (Dieckmann and Hellmer, 2010), which, in turn, provide food for a wide range of heterotrophic organisms (Arrigo, 2014). With Arctic sea ice extent reducing (Meier et al., 2014; Stroeve et al., 2012), there is a need to understand the impact of an associated reduction in sea ice microalgae as they provide an important energy source for the ecosystem (Arrigo, 2014). Fundamental to this understanding is being able to ascertain, quantitatively, the sympagic and pelagic components of an animal's diet. In order for this to be achieved, however, it is first necessary to be able to identify methods by which sympagic and pelagic algae can be both distinguished and quantified. Such methods may, potentially, be available through the identification of signature chemical tracers of each algal type.

Highly branched isoprenoid (HBI) lipids are secondary metabolites that have been reported in a number of marine diatom genera that regularly form components of both sympagic and pelagic algae. For instance, in the Arctic, the sea ice diatoms *Haslea crucigeroides, H. spicula, H. kjellmanii* and *Pleurosigma stuxbergii* var *rhomboides* biosynthesise certain HBIs (e.g. I and III; Fig. 1.; Brown et al., 2014c) that have a distinctive carbon isotopic composition when found in the environment ($\delta^{13}C$ = -19±2‰ and -18±1‰; Belt et al., 2008). While these sympagic HBIs are regularly reported in samples of Arctic sea ice (Belt et al., 2007, 2013; Brown et al., 2011), surface (Belt and Müller, 2013; Navarro-Rodriguez et al., 2013; Smik et al., 2016; Stoynova et al., 2013; Xiao et al., 2015) and downcore (Belt et al., 2015; Müller et al., 2009,2012; Polyak et al., 2016; Stein et al., 2016; Vare et al., 2009) sediments, as yet, they have not been found in pelagic water samples from ice-free locations. In contrast, other HBIs (including, II, IV, V, VI, VII and VIII; Fig. 1) are frequently reported

within pelagic water samples from sub-polar and temperate regions (Belt, et al. 2000; Cooke et al., 1998; Dunlop and Jefferies, 1985; He et al., 2016; Kaiser et al., 2016; Xu et al., 2006), and represent common components of marine sediments worldwide (Belt et al., 2000). These pelagic HBIs have been shown to be biosynthesised by temperate diatoms including *Berkeleya rutilans* (Brown et al., 2014b), *H. ostrearia* (Volkman et al., 1994; Wraige et al., 1997), *Pseudosolenia calcar-avis* (Kaiser et al., 2016), *Pleurosigma intermedium* (Belt et al., 2000; Brown and Belt, 2016), *P. strigosum* (Grossi et al., 2004) and *Rhizosolenia setigera* (Rowland et al., 2001; Volkman et al., 1994), making them ideal indicators of pelagic algae. The HBI biomarker-based H-Print (Brown et al., 2014d) provides a means of numerically combining all of these HBI biomarker abundances into a single index, thereby providing a measure of the relative composition of sympagic and pelagic algae in a sample of mixed content. While end-member H-Print values from sympagic and pelagic algae are relatively straightforward to interpret (Brown et al., 2014a,d), as yet, it has not been established whether intermediate values of the H-Print accurately reflect the relative proportions of mixed sympagic/pelagic algae composition.

The main aim of the current study, therefore, was to identify a numerical model that described the relationship between the H-Print and the proportion of sympagic and pelagic algae for samples created in the laboratory. To achieve this, HBIs were first quantified in a series of samples made by combining varying proportions of both sympagic and pelagic algae. The abundances of various HBI biomarkers were then combined to produce H-Print values, which were subsequently used to establish a regression model. Further, in order to test the applicability of the H-Print approach within an animal grazing context, H-Prints derived from analysis of algal food sources of known composition were compared with those obtained from *Artemia* sp. fed on the same samples.

2 Material and methods

2.1 Diatom composition of sympagic and pelagic algae samples

For the determination of H-Print values in sympagic algae, samples of floating sea ice algae aggregates were used that had been collected from Resolute Bay, Nunavut, Canada (Brown et al., 2014c). Aggregates contained the HBI biosynthesising sea ice diatoms *H. crucigeroides, H. spicula, H. kjellmanii, P. stuxbergii* var *rhomboides* (combined total ca. 2%), with the remainder comprising mainly (ca. 80%) *Navicula pelagica, Pauliella taeniata and Nitzschia frigida* (Brown et al., 2014c). Samples to represent pelagic algae were prepared by combining cultures of known temperate HBI biosynthesising diatom species (*P. intermedium* (ca. 1%), *P. planktonicum* (ca. 0.5%), *P.* sp. (ca. 1%) and *H. ostrearia* (ca. 2%)) with a non-HBI producing centric diatom (*Thalassiosira weisfloggi*; ca. 95%). Total diatom cell abundances in 10 mg subsamples were comparable for both sympagic (3.1 $x10^6$ cell L^{-1}) and pelagic (3.5 $x10^6$ cell L^{-1}) algae.

2.2 Rearing and feeding of *Artemia* sp. - experimental setup

For feeding experiments, *Artemia* sp. were chosen since the *Artemiidae* are considered to be continuous, non-selective filter feeders (Evjemo and Olsen, 1999), reaching saturated ingestion capacity between $2x10^3$ and $1x10^4$ cells L^{-1} (da Costa et al., 2005; Reeve, 1963), which is below the cell abundances used here. About 1000 decapsulated *Artemia* sp. eggs (Waterlife Research ind. Ltd.) were rinsed with deionised water (ca. 10 mL), transferred to 1.5 L clear plastic flasks (Corning) containing artificial seawater with a salinity of 32 (1 L milli-Q water; 32 g TropicMarin® salt), and maintained in suspension by aeration. During

rearing, light intensity was maintained below 1 µmol photons m^{-2} s^{-1}. From 3 days after hatching, a regime of 100% water changes, immediately followed by feeding (ca. 0.5 g H^2Ocean $^{Pro+}$), was carried out every 2–3 days. At >40 days old, 20 individual *Artemia* sp. were selected randomly from the rearing stock and transferred, along with 10 mg algae, to experimental flasks containing artificial seawater. Experimental flasks were maintained at 20±2.5°C and ca. 2 µmol photons m^{-2} s^{-1}, with algae sustained in suspension by vigorous aeration. After feeding on algae for 24 h, *Artemia* sp. were removed from the water using a plastic pipette and pooled (*n*=20) for analysis of HBI content. The remaining water containing ungrazed algae and faecal pellets was filtered (Whatman GF/F) and analysed for HBI content.

2.3 Extraction and analysis of HBI lipids

Extraction of HBI lipids was carried out on algal samples, *Artemia* sp. and filtered water as described previously (Brown et al., 2014a), and the subsequent analysis of purified non-polar extracts containing HBIs was carried out using gas chromatography–mass spectrometry (GC–MS) techniques according to Belt et al. (2012).

2.4 Calculation of the HBI biomarker H-Print

HBI abundances were obtained from GC–MS selective ion monitoring (SIM) output (see Belt et al., 2012) using the mass spectral intensities of the molecular ion for each HBI (Brown et al., 2014d). Individual HBI abundances were normalised according to totals derived from all HBIs. The resulting distribution provided the basis for the H-Print (Brown et al., 2014d), which is defined, here, as the proportion of HBIs from pelagic diatoms relative to those from

both sympagic and pelagic diatoms to provide H-Print values within the range 0–100% (Eq. 1).

Eq. 1.

$$\mathrm{H-Print\ (\%)} = \frac{(\text{pelagic HBIs})}{(\text{sympgaic HBIs} + \text{pelagic HBIs})} \times 100$$

To represent pelagic algae, 4 combinations of HBIs were tested. Firstly, for H-Print[1], all HBI isomers, for which the chemical structures and at least one biological source organism were also known (Eq. 2), were used. For H-Print[2] (Eq. 3), only V and VI were used, since these are the most common HBIs in phytoplankton (Belt et al., 2000). H-Print[3-4] used only V, as it was absent from the sympagic algae (Eq. 4). To represent biomarkers of sympagic algae, I and III were chosen for H-Prints[1-3] (Eq. 2–4) since these are the only HBIs in this study that are known to have a sea ice diatom source (Brown et al., 2014c). For H-Print[4] (Eq. 5) only I was included as a sympagic component since it was not present in the pelagic algae.

Eq. 2.

$$H-Print^{1}\ (\%) = \frac{(\mathrm{II} + \mathrm{IV} + \mathrm{V} + \mathrm{VI} + \mathrm{VII} + \mathrm{VIII})}{(\mathrm{I} + \mathrm{II} + \mathrm{III} + \mathrm{IV} + \mathrm{V} + \mathrm{VI} + \mathrm{VII} + \mathrm{VIII})} \times 100$$

Eq. 3.

$$H-Print^{2}\ (\%) = \frac{(\mathrm{V} + \mathrm{VI})}{(\mathrm{I} + \mathrm{III} + \mathrm{V} + \mathrm{VI})} \times 100$$

Eq. 4.

$$H-Print^{3}\ (\%) = \frac{(\mathrm{V})}{(\mathrm{I} + \mathrm{III} + \mathrm{V})} \times 100$$

Eq. 5

$$H-Print^{4}\ (\%) = \frac{(\mathrm{V})}{(\mathrm{I} + \mathrm{V})} \times 100$$

174

175 2.5 Statistical design

176

177 All experiments were carried out in replicate (*n*=5) and, where *Artemia* sp. were involved,
178 each replicate contained 20 randomly selected individuals, resulting in 100 *Artemia* sp. being
179 used for each treatment. Statistical analysis was performed in R Studio v0.99.441 (R-Core-
180 Team, 2016). ANOVA was used to compare the H-Prints of algae, *Artemia* sp. and filtered
181 water for each treatment. Least squares regression fits were used for comparison of the
182 different H-Print equations across all treatments. Regression models were evaluated on the
183 basis of their ability to predict known algal composition. Predictions of the sympagic algae
184 content of samples based on H-Prints was done using the ‘predict()’ function in base R with
185 confidence intervals of 99%.

186

4 Results

4.1 Quantification of HBIs and H-Prints in algae

Samples of sympagic algae were dominated by HBIs I and III, which comprised 36±5% and 44±5% of total HBIs, respectively (Fig. 2). The remaining HBIs were, individually, all less than 10%, while V and VIII were absent. In contrast, the most abundant HBI in the pelagic algae was V (33±5%), with VI and VII contributing 15±3% and 20±2%, respectively. Other HBIs were each less than 6%, while I and IV were absent from pelagic algae (Fig. 2). For samples consisting exclusively of sympagic algae, calculations using Eq. 2–5 resulted in H-Prints varying between 0–25%, with Eq. 4 and Eq. 5 both giving H-Prints of 0±0%, while Eq. 2 gave the highest values (18±7%). For pelagic algae samples, the variability in H-Print values was much less (97–100%), with Eq. 4 and Eq. 5 providing the lowest (97±1%) and highest (100±0%) values, respectively. For composite samples containing both sympagic and pelagic algae, H-Prints showed more variability than for end-member algae samples. For example, H-Prints from composite samples containing 50% sympagic algae ranged from 42 to 80% with, on average, Eq. 4 giving the lowest (53±8%) values. Highest values were obtained using Eq. 5 (73±7%).

Regression models derived from Eq. 2, 3 and 5 provided estimates of 109–129% sympagic algae for the sympagic end-member sample (Fig. 3, Table 1). The predictive model derived from Eq. 4 estimated the sympagic component to be 101%. For the 50% sympagic algae sample, the models derived from Eq. 2, 3 and 5 gave estimates above the known sympagic contribution (59%, 67% and 61%, respectively), while Eq. 4 predicted 50%. For pelagic end-member samples containing 0% sympagic algae, models using Eq. 2, 3 and 4 all yielded low

H-Prints (4%, 6% and -1% sympagic algae, respectively), while prediction from the model derived using Eq. 5 estimated a 13% contribution from sympagic algae, even though it was absent.

4.2 H-Prints from analysis of *Artemia* sp. and filtered water samples

H-Print data, calculated using Eq. 4, for *Artemia* sp. and filtered water samples were not significantly different from those obtained from algae for any of the sympagic/pelagic compositions used (p = >0.3). Accordingly, almost all of the H-Prints calculated for *Artemia* sp. and filtered water fell well within the 99% confidence interval attached to the model derived from mixed algae (Fig. 4a and 4b).

5. Discussion

5.1 Selection of HBIs for use in the H-Print

In order to make comparisons of food source (as defined by the H-Print) in grazers more achievable, it was necessary to first identify the model that gave the most accurate relationship between H-Prints and the known algal composition. This selection focused on two main criteria; 1) accuracy of estimates and 2) confidence of the model. The most accurate model was derived from H-Print^3 using I, III and V as the constituent HBIs, which estimated the sympagic and pelagic end-members at 101% and -1%, respectively (Table 1). In contrast, models derived from the other H-Prints (1, 2 and 4) overestimated the sympagic component at >109% and >4% for the sympagic and pelagic end-members, respectively. In assessing the confidence intervals of the models, it was also found that the model using H-Print^3 had the smallest mean confidence interval range (29; Table 1), indicating the least uncertainly of all the models, while the remaining models had mean confidence interval ranges >37. The linear model derived from H-Print^3 was therefore used to predict sympagic/pelagic algae composition from hereon.

5.2 Comparison of H-Prints in algae, filtered water and *Artemia* sp.

Having demonstrated that the H-Print could provide reliable estimates of the sympagic/pelagic proportion of mixed algal samples of known composition, it was then necessary to test whether the H-Print could also provide reasonable estimates of the sympagic/pelagic composition of algal food consumed by animals. To be successful, zooplankton needed to feed, non-selectively, upon each algal treatment without alteration of

the H-Print. During the feeding experiments, there were no mortalities of *Artemia* sp., and the consistent, rapid appearance of visible faecal pellets indicated that non-selective grazing occurred for all experimental treatments. Experiments were run over 24 h to give *Artemia* sp. suitable opportunity to consume algae, and it is estimated that *Artemia* sp. consumed ca. 150% of the available algae during each experiment. This was determined by comparing the amount of HBI I in the 10 mg sympagic algae supplied to *Artemia* sp. (ca. 0.59 µg), with that in pooled *Artemia* sp. after 24 h (ca. 0.02 µg), which indicated that ca. 3% of the algae was present in the guts of *Artemia* sp. Based on an assumption of a gut passage time of 20–30 minutes (Nimura, 1989), it is estimated that ca. 50 gut passages per individual (ca. 1000 for 20 individuals) occurred over the duration of each experiment, potentially resulting in 15 mg (150%) algae being consumed. This outcome is supported by the experiments of Reeve (1963) who showed that *Artemia* sp. consumed *Phaeodactylum tricornutum* at ca. $4x10^5$ cells h^{-1}, which, over 24 h, corresponds to ca. 300% of our 3.1 $x10^6$ cell L^{-1}, and seems quite feasible given the tendency for coprophagy in captive zooplankton (Werner, 2000). Despite the efficient grazing of sympagic algae in the current experiments, *Artemia* sp. did not alter the relative distributions of individual HBI biomarkers. Indeed, the majority (80%) of mean H-Prints derived from water and *Artemia* sp. fell within the 99% confidence interval of the regression model calculated using the algal H-Print^3 (Fig. 4b), suggesting that *Artemia* sp. grazed non-selectively on all treatments, without alteration of the H-Print. It is concluded, therefore, that the regression model, based upon algal H-Prints, remains accurate for *Artemia* sp., permitting application of the regression model to predict the sympagic/pelagic proportion of zooplankton diet.

5.3 Environmental application of the H-Print

Although it has been shown here that the H-Print approach can yield reliable estimates of the sympagic/pelagic composition of algae in the laboratory, even after being consumed by zooplankton, it is probably also important to consider some additional factors that may be important when using this method in environmental settings in the future. Three such factors are considered briefly here. Firstly, HBIs should be readily detectable in the environment. Recently, the ubiquity of HBIs has been established following the widespread reporting of these lipids in, for example, sea ice (Belt et al., 2007,2013,2016; Brown et al., 2011; Massé et al., 2011; Nichols et al., 1988), sediments (Belt and Müller, 2013; Navarro-Rodriguez et al., 2013; Xiao et al., 2015), zooplankton (Brown and Belt, 2012; Cripps, 1995), fish (Brown et al., 2015; Goutte et al., 2014b), birds (Brown et al., 2013a,2015) and marine mammals (Brown, et al., 2013a,2014a; Goutte et al., 2014a) from Arctic, Antarctic and temperate environments. Second, it is suggested that identification of the H-Print formula that best reflects the composition of natural sympagic and pelagic algae may also be important. In the current study, it was shown that a key factor in identifying such a formula was selection of HBIs that provide a balanced contribution from sympagic and pelagic sources. Achieving this balance is, to some extent, simplified by the shared ability of sympagic and pelagic algae to biosynthesise HBIs, thereby minimising any potential complications associated with comparing lipids from different sources; a problem frequently associated with more common lipids such as fatty acids or sterols which can have a wide range of sources (e.g. Natalia et al., 1999; Volkman et al., 1986,1998), including, in some cases, animals themselves. Nonetheless, the proportion of sympagic/pelagic HBIs will be dependent upon the overall abundances of HBI-biosynthesising diatoms present. On this basis, it is anticipated that H-Print^3 may, as it did in the experiments described herein, provide the most realistic estimates for environmental samples, since the species known to produce I, III and V have similar abundances in the environment. For example, the diatoms that produce I and III have a

299 consistent abundance in sea ice throughout the Arctic (1–5%; Brown et al., 2014c and
300 references therein), while *Pleurosigma* spp. and *Rhizosolenia* spp. (known sources of V) are
301 also typically 1–5% of species in pelagic diatom assemblages (Mather et al., 2010; von
302 Quillfeldt, 2000). On the other hand, if the abundances of the sympagic or pelagic sources
303 should differ substantially from this, it is possible that H-Print^3 may not be the best predictor
304 of algal composition and a different combination of HBIs may give more reliable estimates.
305 In order to obtain the most reliable estimates of algal composition in samples collected from
306 the environment, it is therefore recommended that H-Prints for both sympagic and pelagic
307 algae are determined on a case-by-case basis using samples collected from the environment
308 being studied. Accordingly, the appropriate model can thus be selected that best estimates the
309 composition of mixed algae samples.
310
311 Finally, differential modification of HBI lipid distributions within animals would likely result
312 in inaccurate estimates of algae composition, regardless of which H-Print formula is used. As
313 such, it is important that, once consumed by animals, HBIs do not become modified from
314 their original source distributions, as was the case for *Artemia* sp. described herein. In the
315 Arctic, the most abundant zooplankton are usually *Calanus* spp. (Auel and Hagen, 2002;
316 Søreide et al., 2008) and, in contrast to *Artemia* sp., these do accumulate lipids (Graeve et al.,
317 2005; Pond and Tarling, 2011). The close similarity of *Calanus* spp. H-Prints with those from
318 pelagic algae (Brown et al., 2014d), however, in addition to those between some higher
319 trophic level organisms and sympagic algae (Brown et al., 2014d), suggest that HBI
320 distributions are not noticeably impacted by animals. Indeed, quantitative assessment of the
321 relative proportions of I and III in over 300 ringed seals showed a consistent ratio (1:2.7) that
322 aligned closely to typical values from sea ice (e.g. 1:2.1 (Belt et al., 2013) and 1:2.9 (Brown,
323 2011)), further supporting the finding here that H-Prints are unlikely to be significantly

altered by animals. Confirmation of this, however, will likely require further analyses of larger sample sets that focus on Arctic animals feeding on prey with known H-Print signatures.

In summary, the data presented herein demonstrate that the biomarker-based H-Print has the potential to provide reliable, quantitative predictions of the sympagic/pelagic composition of animal diet. This conclusion is based upon a series of controlled laboratory experiments from which, first, a linear regression model was created, where H-print values reflected the relative proportions of sympagic and pelagic algae in mixtures of known composition. In addition, there was no significant difference in the numerical values of H-Prints measured in these samples of mixed algae and in zooplankton that had been fed these food sources. The potential for the H-Print method to provide quantitative estimates of the role that sympagic algae play in animal diet will likely lead to valuable new field data for modelling the broader ecological impacts of reducing Arctic sea ice extent.

Acknowledgements

This work was supported by a Leverhulme Trust Research Project Grant (RPG-2014-021). The authors also thank Sandra Shumway and an anonymous reviewer for providing supportive feedback on the manuscript.

344 References

345 Arrigo, K.R., 2014. Sea Ice Ecosystems. Ann. Rev. Mar. Sci. 6, 439–467.

346 Auel, H., Hagen, W., 2002. Mesozooplankton community structure, abundance and biomass
347 in the central Arctic Ocean. Mar. Biol. 140, 1013–1021.

348 Belt, S.T., Müller, J., 2013. The Arctic sea ice biomarker IP_{25}: a review of current
349 understanding, recommendations for future research and applications in palaeo sea ice
350 reconstructions. Quat. Sci. Rev. 79, 9–25.

351 Belt, S.T., Allard, W.G., Massé, G., Robert, J.M., Rowland, S.J., 2000. Highly branched
352 isoprenoids (HBIs): Identification of the most common and abundant sedimentary
353 isomers. Geochim. Cosmochim. Acta 64, 3839–3851.

354 Belt, S.T., Massé, G., Rowland, S.J., Poulin, M., Michel, C., LeBlanc, B., 2007. A novel
355 chemical fossil of palaeo sea ice: IP_{25}. Org. Geochem. 38, 16–27.

356 Belt, S.T., Massé, G., Vare, L.L., Rowland, S.J., Poulin, M., Sicre, M.-A., Sampei, M.,
357 Fortier, L., 2008. Distinctive ^{13}C isotopic signature distinguishes a novel sea ice
358 biomarker in Arctic sediments and sediment traps. Mar. Chem. 112, 158–167.

359 Belt, S.T., Brown, T.A., Navarro-Rodriguez, A., Cabedo-Sanz, P., Tonkin, A., Ingle, R.,
360 2012. A reproducible method for the extraction, identification and quantification of
361 the Arctic sea ice proxy IP_{25} from marine sediments. Anal. Methods 4, 705–713.

362 Belt, S.T., Brown, T.A., Ringrose, A.E., Cabedo-Sanz, P., Mundy, C.J., Gosselin, M., Poulin,
363 M., 2013. Quantitative measurement of the sea ice diatom biomarker IP_{25} and sterols
364 in Arctic sea ice and underlying sediments: further considerations for palaeo sea ice
365 reconstruction. Org. Geochem. 62, 33–45.

366 Belt, S.T., Cabedo-Sanz, P., Smik, L., Navarro-Rodriguez, A., Berben, S.M.P., Knies, J.,
367 Husum, K., 2015. Identification of paleo Arctic winter sea ice limits and the marginal

ice zone: Optimised biomarker-based reconstructions of late Quaternary Arctic sea ice. Earth Planet. Sci. Lett. 431, 127–139.

Belt, S.T., Smik, L., Brown, T.A., Kim, J.-H., Rowland, S.J., Allen, C.S., Gal, J.-K., Shin, K.-H., Lee, J.I., Taylor, K.W.R., 2016. Source identification and distribution reveals the potential of the geochemical Antarctic sea ice proxy $IPSO_{25}$. Nat. Commun. 7,12655.

Brown, T.A., 2011. Production and preservation of the Arctic sea ice diatom biomarker IP_{25}. PhD Thesis, School of Geography Earth and Environmental Sciences. University of Plymouth, Plymouth.

Brown, T.A., Belt, S.T., Philippe, B., Mundy, C.J., Massé, G., Poulin, M., Gosselin, M., 2011. Temporal and vertical variations of lipid biomarkers during a bottom ice diatom bloom in the Canadian Beaufort Sea: Further evidence for the use of the IP_{25} biomarker as a proxy for spring Arctic sea ice. Polar Biol. 34, 1857–1868.

Brown, T.A., Belt, S.T., 2012. Closely linked sea ice–pelagic coupling in the Amundsen Gulf revealed by the sea ice diatom biomarker IP_{25}. J. Plankton Res. 34, 647–654.

Brown, T.A., Belt, S.T., Ferguson, S.H., Yurkowski, D.J., Davison, N.J., Barnett, J.E.F., Jepson, P.D., 2013a. Identification of the sea ice diatom biomarker IP_{25} and related lipids in marine mammals: A potential method for investigating regional variations in dietary sources within higher trophic level marine systems. J. Exp. Mar. Biol. Ecol. 441, 99–104.

Brown, T.A., Bicknell, A.W.J., Votier, S.C., Belt, S.T., 2013b. Novel molecular fingerprinting of marine avian diet provides a tool for gaining insights into feeding ecology. Environ. Chem. Lett. 11, 283–288.

Brown, T.A., Alexander, C., Yurkowski, D.J., Ferguson, S., Belt, S.T., 2014a. Identifying variable sea ice carbon contributions to the Arctic ecosystem: A case study using

highly branched isoprenoid lipid biomarkers in Cumberland Sound ringed seals. Limnol. Oceanogr. 59, 1581–1589.

Brown, T.A., Belt, S.T., Cabedo-Sanz, P., 2014b. Identification of a novel di-unsaturated C_{25} highly branched isoprenoid in the marine tube-dwelling diatom *Berkeleya rutilans*. Environ. Chem. Lett. 12, 455–460.

Brown, T.A., Belt, S.T., Tatarek, A., Mundy, C.J., 2014c. Source identification of the Arctic sea ice proxy IP_{25}. Nat. Commun. 5, 4197.

Brown, T.A., Yurkowski, D.J., Ferguson, S.H., Alexander, C., Belt, S.T., 2014d. H-Print: a new chemical fingerprinting approach for distinguishing primary production sources in Arctic ecosystems. Environ. Chem. Lett. 12, 387–392.

Brown, T.A., Hegseth, E.N., Belt, S.T., 2015. A biomarker-based investigation of the mid-winter ecosystem in Rijpfjorden, Svalbard. Polar Biol. 38, 37–50.

Brown, T.A., Belt, S.T., 2016. Novel tri- and tetra-unsaturated highly branched isoprenoid (HBI) alkenes from the marine diatom *Pleurosigma intermedium*. Org. Geochem. 91, 120–122.

Cooke, D.A., Barlow, R., Green, J., Belt, S.T., Rowland, S.J., 1998. Seasonal variations of highly branched isoprenoid hydrocarbons and pigment biomarkers in intertidal sediments of the Tamar Estuary, UK. Mar. Environ. Res. 45, 309–324.

Cripps, G.C., 1995. The occurrence of monounsaturated n-C_{21} and polyunsaturated C_{25} sedimentary hydrocarbons in the lipids of Antarctic marine organisms. Polar Biol. 15, 253–259.

da Costa, R.A.A.M., Koening, M.L., Pereira, L.C.C., 2005. Feeding adult of *Artemia salina* (Crustacea-Branchiopoda) on the dinoflagellate *Gyrodinium corsicum* (Gymnodiniales) and the Chryptophyta *Rhodomonas baltica*. Braz. Arch. Biol. Technol. 48, 581–587.

418 Dieckmann, G.S., Hellmer, H.H., 2010. The importance of sea ice: An overview. In: Thomas,
419 D., Dieckmann, S. (Eds.), Sea ice (second edition). Blackwell Publishing, Chichester,
420 pp. 1–22.
421 Dunlop, R.W., Jefferies, P.R., 1985. Hydrocarbons of the hypersaline basins of Shark Bay,
422 Western-Australia. Org. Geochem. 8, 313–320.
423 Evjemo, J.O., Olsen, Y., 1999. Effect of food concentration on the growth and production
424 rate of *Artemia franciscana* feeding on algae (T. iso). J. Exp. Mar. Biol. Ecol. 242,
425 273–296.
426 Goutte, A., Charrassin, J.B., Cherel, Y., Carravieri, A., De Grissac, S., Masse, G., 2014a.
427 Importance of ice algal production for top predators: new insights using sea-ice
428 biomarkers. Mar. Ecol. Prog. Ser. 513, 269–275.
429 Goutte, A., Cherel, Y., Ozouf-Costaz, C., Robineau, C., Lanshere, J., Massé, G., 2014b.
430 Contribution of sea ice organic matter in the diet of Antarctic fishes: a diatom-specific
431 highly branched isoprenoid approach. Polar Biol. 37, 903–910.
432 Graeve, M., Albers, C., Kattner, G., 2005. Assimilation and biosynthesis of lipids in Arctic
433 Calanus species based on feeding experiments with a ^{13}C labelled diatom. J. Exp.
434 Mar. Biol. Ecol. 317, 109–125.
435 Grossi, V., Beker, B., Geenevasen, J.A.J., Schouten, S., Raphel, D., Fontaine, M.-F.,
436 Sinninghe Damsté, J.S., 2004. C_{25} highly branched isoprenoid alkene from the marine
437 benthic diatom *Pleurosigma strigosum*. Phytochemistry 65, 3049–3055.
438 He, D., Simoneit, B.R.T., Xu, Y., Jaffé, R., 2016. Occurrence of unsaturated C_{25} highly
439 branched isoprenoids (HBIs) in a freshwater wetland. Org. Geochem. 93, 59–67.
440 Kaiser, J., Belt, S.T., Tomczak, M., Brown, T.A., Wasmund, N., Arz, H.W., 2016. C_{25} highly
441 branched isoprenoid alkenes in the Baltic Sea produced by the marine planktonic
442 diatom *Pseudosolenia calcar-avis*. Org. Geochem. 93, 51–58.

443 Massé, G., Belt, S.T., Crosta, X., Schmidt, S., Snape, I., Thomas, D.N., Rowland, S.J., 2011.
444 Highly branched isoprenoids as proxies for variable sea ice conditions in the Southern
445 Ocean. Antarct. Sci. 23, 487–498.
446 Mather, L., MacIntosh, K., Kaczmarska, I., Klein, G., Martin, J.L., 2010. A checklist of
447 diatom species reported (and presumed native) from Canadian coastal waters. Can.
448 Tech. Rep. Fish. Aquat. Sci. 1–78.
449 Meier, W.N., Hovelsrud, G.K., van Oort, B.E.H., Key, J.R., Kovacs, K.M., Michel, C., Haas,
450 C., Granskog, M.A., Gerland, S., Perovich, D.K., Makshtas, A., Reist, J.D., 2014.
451 Arctic sea ice in transformation: A review of recent observed changes and impacts on
452 biology and human activity. Rev. Geophys. 2013RG000431.
453 Müller, J., Massé, G., Stein, R., Belt, S.T., 2009. Variability of sea-ice conditions in the Fram
454 Strait over the past 30,000 years. Nat. Geosci. 2, 772–776.
455 Müller, J., Werner, K., Stein, R., Fahl, K., Moros, M., Jansen, E., 2012. Holocene cooling
456 culminates in sea ice oscillations in Fram Strait. Quat. Sci. Rev. 47, 1–14.
457 Natalia, V. Z., and I. K. Vladimir. 1999. Sources of essential fatty acids in the marine
458 microbial loop. Aquat. Microb. Ecol. 17, 153–157.
459 Navarro-Rodriguez, A., Belt, S.T., Knies, J., Brown, T.A., 2013. Mapping recent sea ice
460 conditions in the Barents Sea using the proxy biomarker IP_{25}: implications for palaeo
461 sea ice reconstructions. Quat. Sci. Rev. 79, 26–39.
462 Nichols, P.D., Palmisano, A.C., Volkman, J.K., Smith, G.A., White, D.C., 1988. Occurrence
463 of an isoprenoid C_{25} diunsaturated alkene and high neutral lipid content in Antarctic
464 sea-ice diatom communities. J. Phycol. 24, 90–96.
465 Nimura, Y., 1989. Shortest gut passage time and gut content volume of *Artemia franciscana*.
466 Nippon Suisan Gakkaishi 55, 2209–2209.

Polyak, L., Belt, S.T., Cabedo-Sanz, P., Yamamoto, M., Park, Y.-H., 2016. Holocene sea-ice conditions and circulation at the Chukchi-Alaskan margin, Arctic Ocean, inferred from biomarker proxies. Holocene 26, 1810–1821.

Pond, D.W., Tarling, G.A., 2011. Phase transitions of wax esters adjust buoyancy in diapausing Calanoides acutus. Limnol. Oceanogr. 56, 1310–1318.

R-Core-Team, 2016. R: A language and environment for statistical computing, R Foundation for Statistical Computing, Vienna, Austria, pp. URL http://www.R-project.org/.

Reeve, M.R., 1963. The Filter-Feeding of Artemia. I. In Pure Cultures of Plant Cells 40, 195–205.

Rowland, S.J., Allard, W.G., Belt, S.T., Massé, G., Robert, J.M., Blackburn, S., Frampton, D., Revill, A.T., Volkman, J.K., 2001. Factors influencing the distribution of polyunsaturated terpenoids in the diatom, *Rhizosolenia setigera*. Phytochemistry 58, 717–728.

Smik, L., Cabedo-Sanz, P., Belt, S.T., 2016. Semi-quantitative estimates of paleo Arctic sea ice concentration based on source-specific highly branched isoprenoid alkenes: A further development of the PIP_{25} index. Org. Geochem. 92, 63–69.

Søreide, J.E., Falk-Petersen, S., Hegseth, E.N., Hop, H., Carroll, M.L., Hobson, K.A., Blachowiak-Samolyk, K., 2008. Seasonal feeding strategies of Calanus in the high-Arctic Svalbard region. Deep-Sea Res. Pt. II 55, 2225–2244.

Stein, R., Fahl, K., Schreck, M., Knorr, G., Niessen, F., Forwick, M., Gebhardt, C., Jensen, L., Kaminski, M., Kopf, A., Matthiessen, J., Jokat, W., Lohmann, G., 2016. Evidence for ice-free summers in the late Miocene central Arctic Ocean. Nat. Commun. 7, 11148.

Stoynova, V., Shanahan, T.M., Hughen, K.A., de Vernal, A., 2013. Insights into Circum-Arctic sea ice variability from molecular geochemistry. Quat. Sci. Rev. 79, 63–73.

Stroeve, J.C., Kattsov, V., Barrett, A., Serreze, M., Pavlova, T., Holland, M., Meier, W.N., 2012. Trends in Arctic sea ice extent from CMIP5, CMIP3 and observations. Geophys. Res. Lett. 39.

Vare, L.L., Massé, G., Gregory, T.R., Smart, C.W., Belt, S.T., 2009. Sea ice variations in the central Canadian Arctic Archipelago during the Holocene. Quat. Sci Rev. 28, 1354–1366.

Volkman, J. K. 1986. A review of sterol markers for marine and terrigenous organic matter. Org. Geochem. 9, 83–99.

Volkman, J. K., Barrett, S.M., Blackburn, S.I., Mansour, M.P., Sikes, E.L., Gelin, F., 1998. Microalgal biomarkers: A review of recent research developments. Org. Geochem. 29, 1163–1179.

Volkman, J.K., Barrett, S.M., Dunstan, G.A., 1994. C_{25} and C_{30} highly branched isoprenoid alkenes in laboratory cultures of two marine diatoms. Organic Geochemistry 21, 407-414.

von Quillfeldt, C.H., 2000. Common Diatom Species in Arctic Spring Blooms: Their Distribution and Abundance, Botanica Marina, pp. 499.

Werner, I., 2000. Faecal pellet production by Arctic under-ice amphipods–transfer of organic matter through the ice/water interface. Hydrobiologia 426, 89–96.

Wraige, E.J., Belt, S.T., Lewis, C.A., Cooke, D.A., Robert, J.M., Massé, G., Rowland, S.J., 1997. Variations in structures and distributions of C_{25} highly branched isoprenoid (HBI) alkenes in cultures of the diatom, *Haslea ostrearia* (Simonsen). Org. Geochem. 27, 497–505.

Xiao, X., Fahl, K., Müller, J., Stein, R., 2015. Sea-ice distribution in the modern Arctic Ocean: Biomarker records from trans-Arctic Ocean surface sediments. Geochim. Cosmochim. Acta 155, 16–29.

517 Xu, Y., Jaffé, R., Wachnicka, A., Gaiser, E.E., 2006. Occurrence of C_{25} highly branched
518 isoprenoids (HBIs) in Florida Bay: Paleoenvironmental indicators of diatom-derived
519 organic matter inputs. Org. Geochem. 37, 847–859.

520

521

522

523 Table 1. Estimates of the sympagic contribution to mixed sympagic/pelagic algae samples

	H-Print Eq.#	***R^2***	***Residual (se)***	***df***	***p***	**Model estimates of sympagic contribution (95% CI) to composite algae**			**Mean CI range**
Composition (S:P)						0:100	50:50	100:0	
H-Print[1]	2	0.95	8.6	23	<0.01	4 (-14 – 23)	59 (41 – 77)	113 (95 – 133)	37
H-Print[2]	3	0.92	10.4	23	<0.01	6 (-16 – 29)	67 (45 – 89)	129 (104 – 153)	46
H-Print[3]	4	0.97	6.6	23	<0.01	-1 (-16 – 14)	50 (36 – 64)	101 (87 – 116)	29
H-Print[4]	5	0.89	11.7	23	<0.01	13 (-11 – 39)	61 (37 – 86)	109 (83 – 135)	50

524

525

526 Figure legends

527 Figure 1. Structures of diatom highly branched isoprenoid (HBI) lipid biomarkers described
528 in this study.

529

530 Figure 2. Relative proportions of highly branched isoprenoids (HBIs) in sympagic and
531 pelagic algae used in this study.

532

533 Figure 3. Mean H-Print (±SE) of algae samples containing sympagic and pelagic algae
534 calculated using Eq. 2-5. Horizontal dashed lines show mean H-Prints calculated for samples
535 containing 50% sympagic and 50% pelagic algae. Solid coloured lines are linear least squares
536 regression fits to data points for each H-Print.

537

538 Figure 4. a) Mean H-Print^3 (±SE) of algae samples containing sympagic and pelagic algae.
539 Straight line (R^2 = 0.97; p = <0.001) regression fit using H-Print^3 of food with 0.99
540 confidence interval (SE) with regression formula shown. Horizontal and vertical dashed lines
541 refer to 50:50 sympagic:pelagic and 50% H-Print. b) Mean H-Print^3 (±SE) of *Artemia* sp.
542 (triangles) and filtered water (down triangles) calculated with H-Print^3. Shaded area shows
543 upper and lower CI from H-Print^3 algae regression model from panel a.

544

545

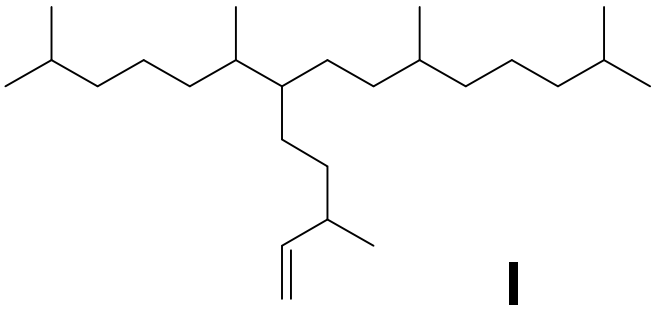

I

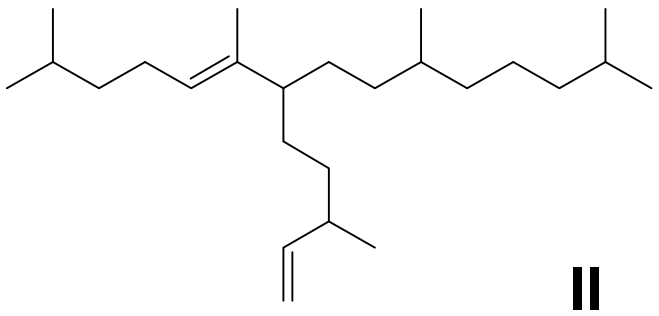

II

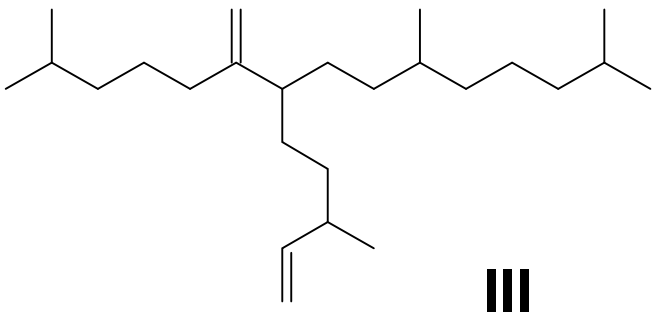

III

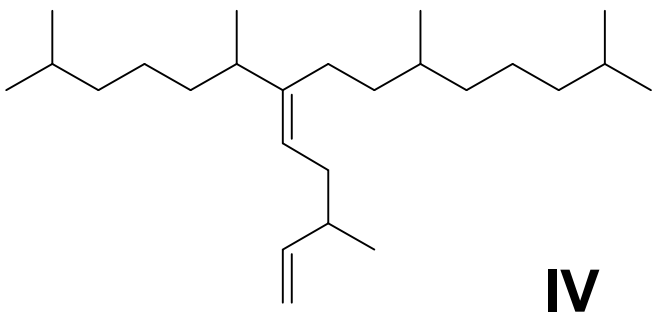

IV

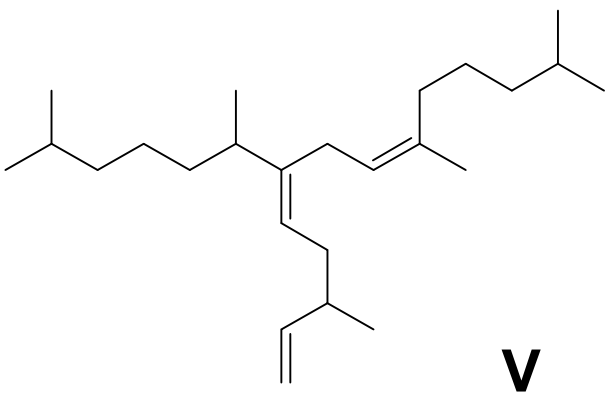

V

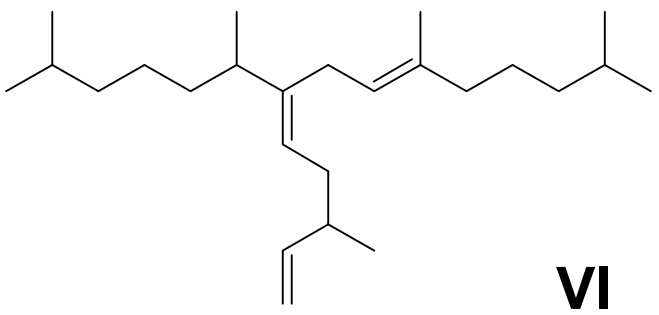

VI

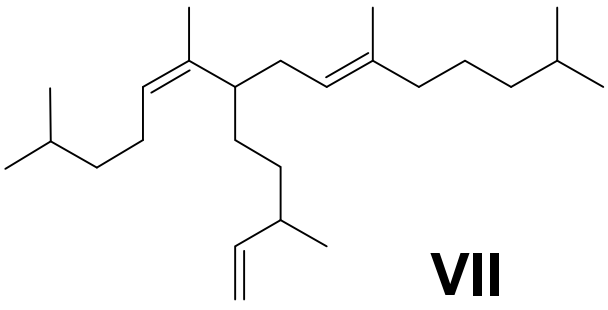

VII

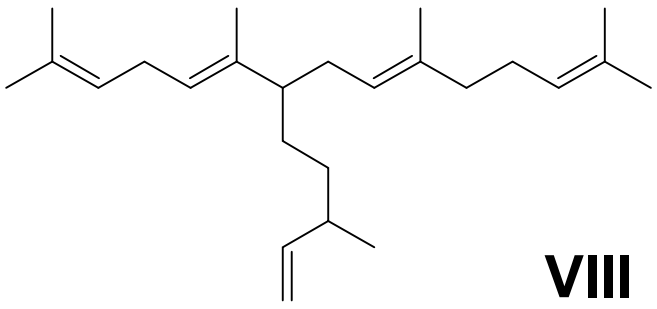

VIII